Atomic insight into hydration shells around facetted nanoparticles

Thomä et al.

Supplementary Figures

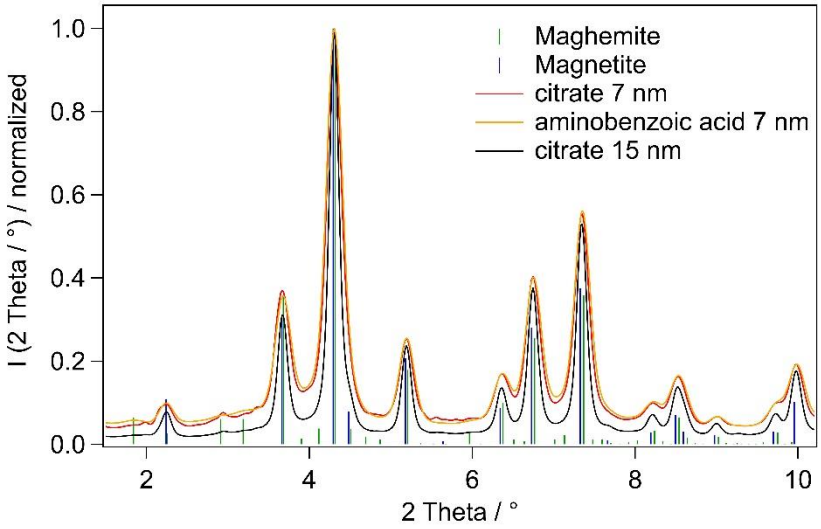

Supplementary Figure 1| XRD data of iron oxide nanopowders (IONP). Background corrected XRD data of water-dispersible IONPs in comparison to XRD reference patterns of magnetite and maghemite. The peak broadening coincides with particle sizes determined from TEM and DLS and is indicative for the nanocrystalline nature of the samples. Both reference patterns match the data very well. Due to the broad peaks and increased background from the nanoparticles it cannot be assured that phase pure magnetite (as intended) was synthesized. Maghemite reflections may be hidden in the background. Presence of a minor maghemite phase is proposed to be likely, since presence of oxygen during synthesis cannot be excluded.

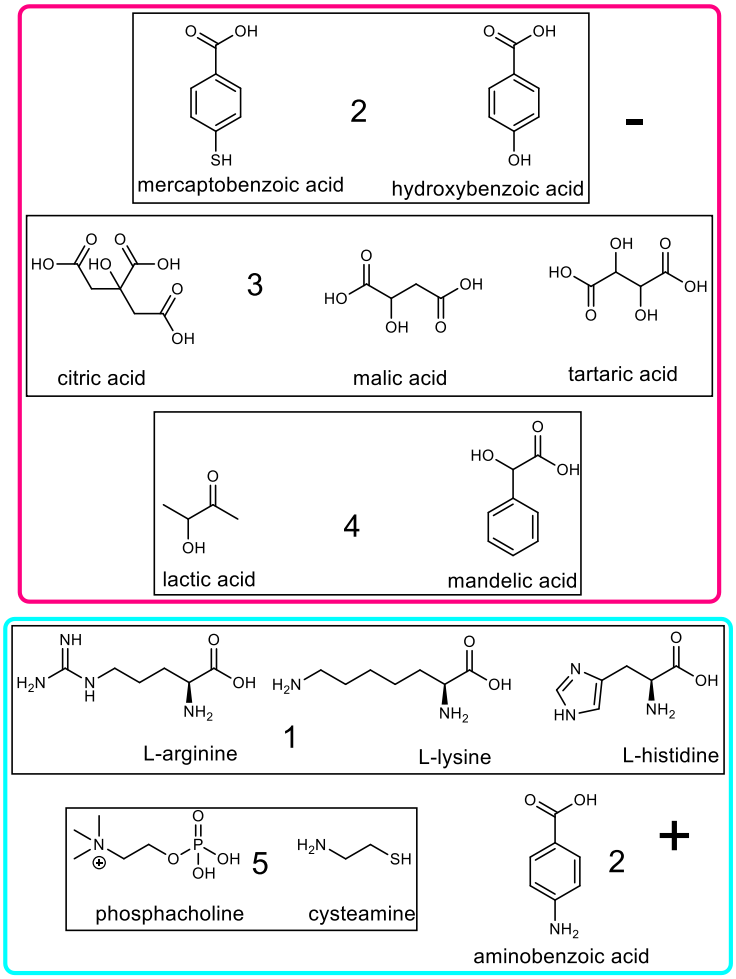

Supplementary Figure 2 | Molecular formulas of ligands grouped according to functional groups. Group 1 are basic amino acids, group 2 benzoic acids, group 3 dibutanoic acids, group 4 small α-hydroxy acids and group 5 two other bifunctional molecules. Iron oxide nanoparticles (IONPs) capped with the molecules in the magenta coloured box are dispersed in basic water and exhibit negative zetapotential. IONPs capped with the molecules in the blue coloured box are dispersed in acidic (or Milli-Q) water and exhibit positive zetapotential.

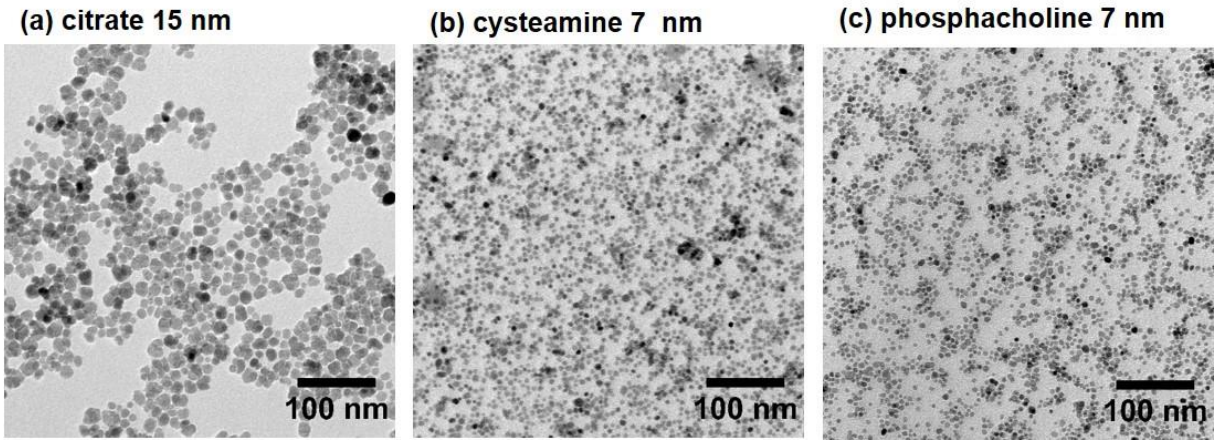

Supplementary Figure 3| TEM images of iron oxide nanoparticles (IONPs). Exemplary TEM images of differently capped water-dispersible IONPs of two different sizes. (a) citrate-capped 15 nm IONPS. (b) cysteamine-capped 7 nm IONPs. (c) phosphacholine-capped 7 nm IONPs.

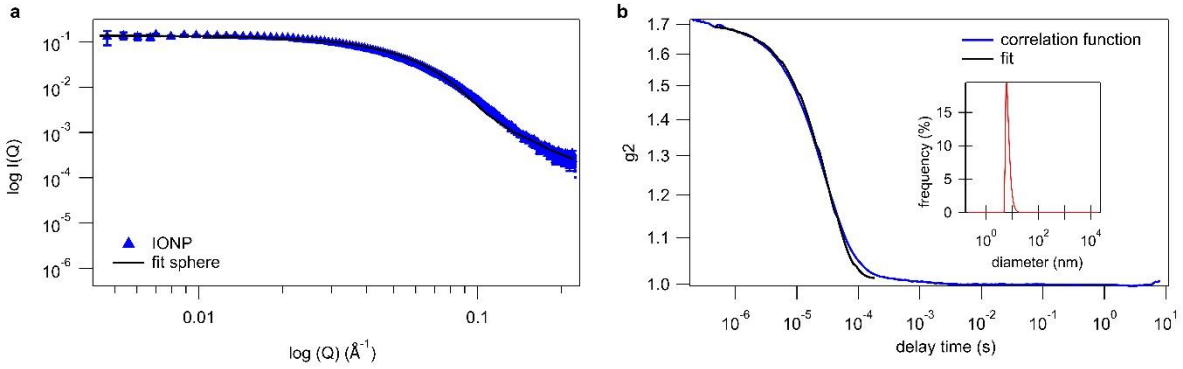

Supplementary Figure 4 | Exemplary SAXS and DLS data of cysteamine-capped iron oxide nanoparticle dispersion. a, The Figure shows an exemplary SAXS measurement of cysteamine-capped IONPs of about 7 nm in diameter. The fit for a sphere with diameter 6 ± 1.8 nm describes the SAXS data very well. **b,** The intensity auto-correlation function of the same sample measured with a Particle Analyzer Lite 500 and the provided fit are shown. The number-weighted average size of this measurement is 7.1 nm (average of three measurements 7.0 ± 0.2). The number-weighted average size distribution is depicted in the inset.

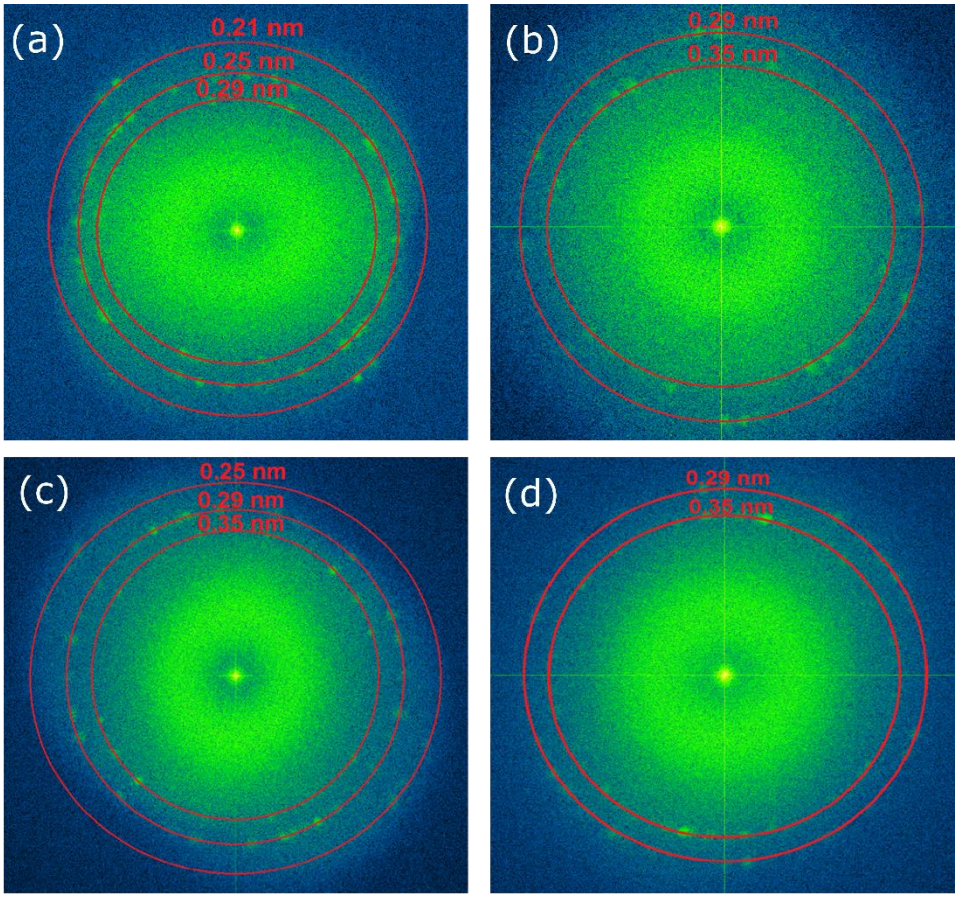

Supplementary Figure 5| TEM diffraction images of iron oxide nanoparticles (IONPs). (a) L-lysine. (b) aminobenzoic acid. (c) cysteamine. (d) tartaric acid. The diffraction images were created with Fourier Transformation of TEM images of the lattice planes of IONPs. From projections of magnetite facets in Jmole, occurring atomic distances in those facets can be identified. These are 0.21 and 0.29 nm for (100), 0.21, 0.24 and 0.29 for (110) and 0.29 and 0.35 nm for (111) facets.

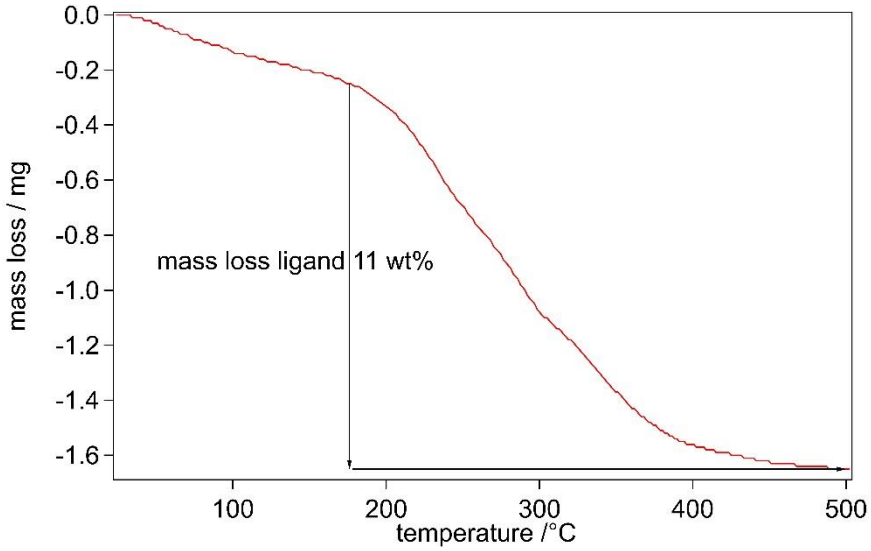

Supplementary Figure 6 | TGA data for hydroxybenzoic acid-capped iron oxide nanoparticles (IONPs). The mass loss during TGA measurement dependent on the temperature. After all surface-bound water is evaporated the organic ligand is thermally decomposed. With the mass loss over ca. 160°C and the particle size ligand coverage per surface area was calculated based from the mass loss and particle size.

Surface coverage [nm^{-2}] = $\frac{V_{NP}\rho N_A n_{ligand}}{m_{NP,TGA}A_{NP}}$

with V_{NP}, A_{NP} as volume and surface area of the nanoparticle, N_A the Avogadro constant, $m_{NP,TGA}$ the mass of the IONPs in the TGA measurement and n_{ligand} the mole number of ligand molecules calculated from the mass loss in TGA via $\Delta m_{ligand}/m_{ligand}$ where M_{ligand} is the molar mass of the ligand.

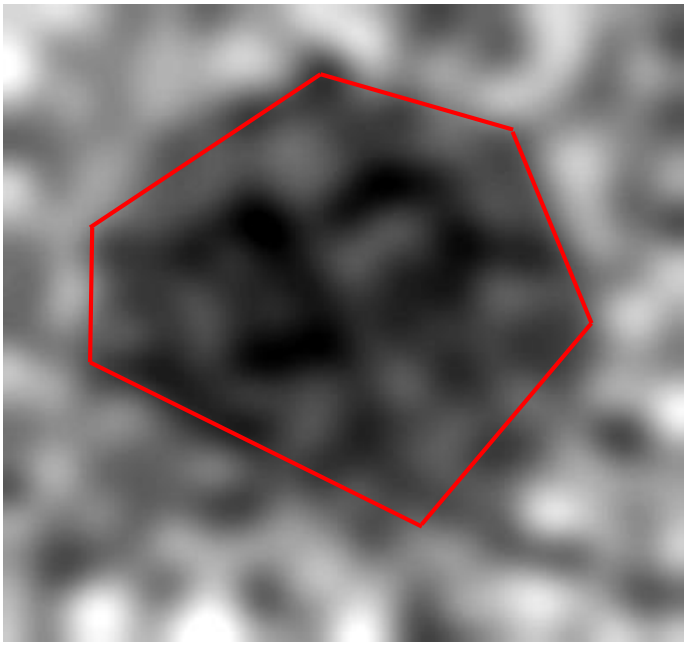

Supplementary Figure 7 | TEM image of facetted L-lysine-capped iron oxide nanoparticles. The exemplary TEM image in high magnification clearly shows, that the IONPs are not spherical, but facetted.

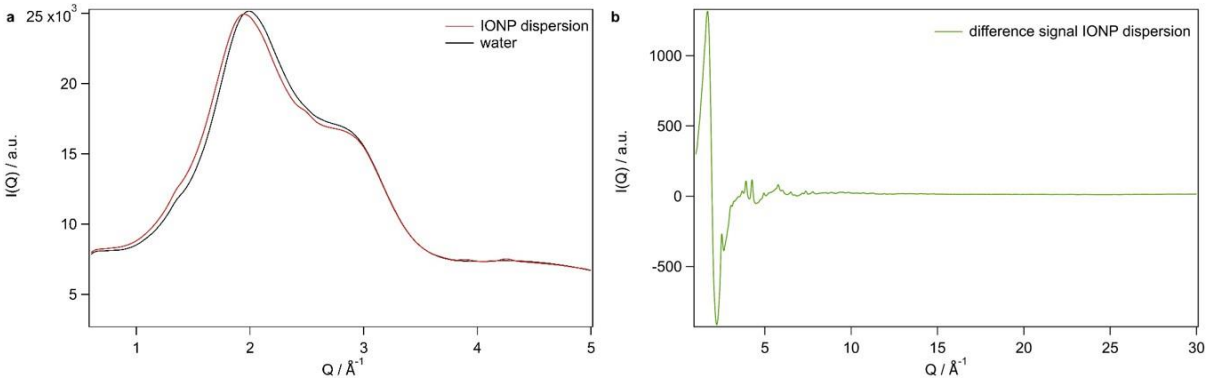

Supplementary Figure 8 | Shift of the FSDP of iron oxide nanoparticle (IONP) dispersion and difference signal. a, The FSDP of the IONP dispersion is shifted in comparison to water from 1.99 $Å^{-1}$ to 1.94 $Å^{-1}$. **b,** Resulting I(Q) difference signal of IONP dispersion contains information about the shift as well as signal arising due to Bragg reflections of the NPs.

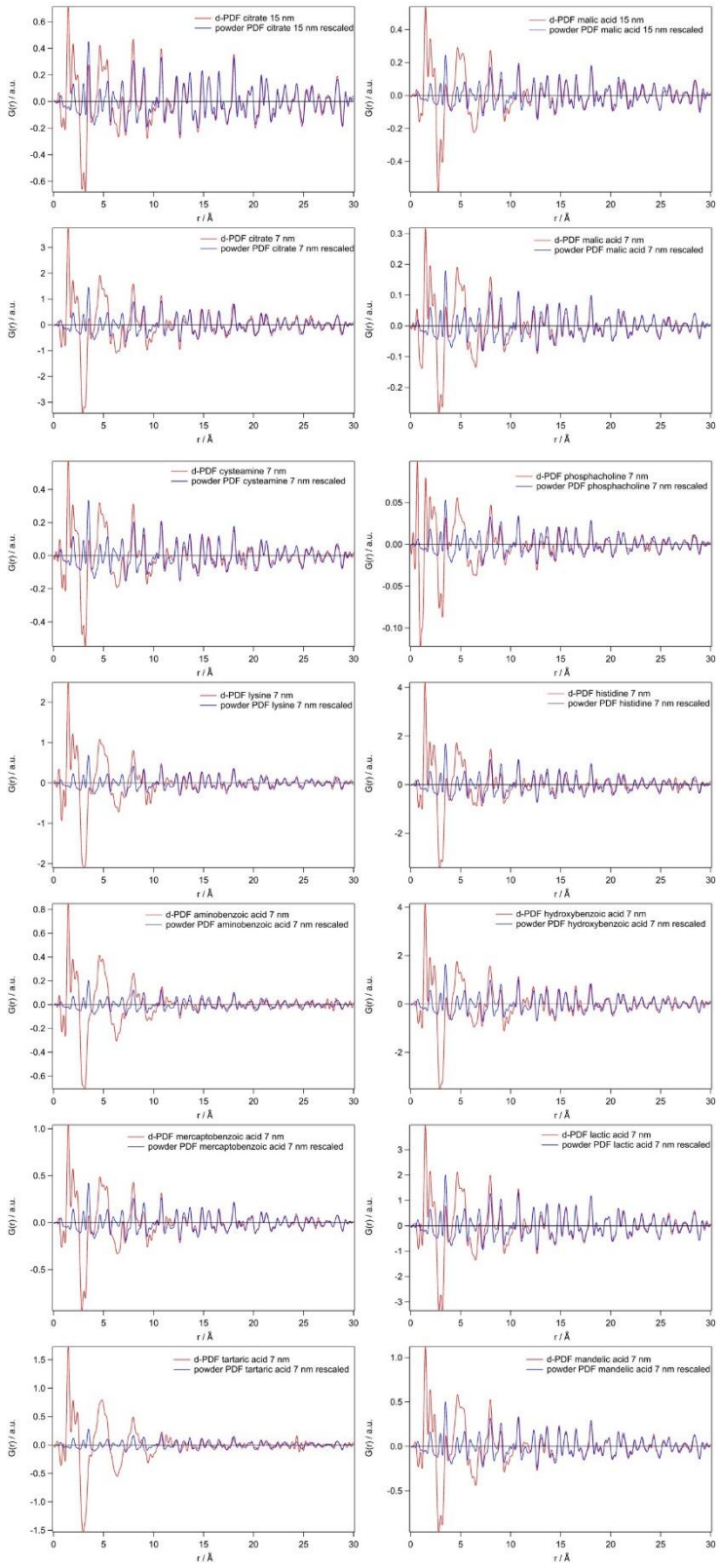

Supplementary Figure 9| Difference pair distribution functions (d-PDF) of all samples with their corresponding scaled powder PDFs. All d-PDFs (except arginine-capped IONP dispersion see main article) are shown with the corresponding scaled powder PDF. For distances larger than 15 $Å^{-1}$ the experimental powder PDFs match the d-PDFs perfectly well. For lower distances the d-PDF differs from the powder PDFs due to build hydration shell around the NPs. The restructured water oscillates around the powder PDFs. For resulting dd-PDFs see Supplementary Figure 12.

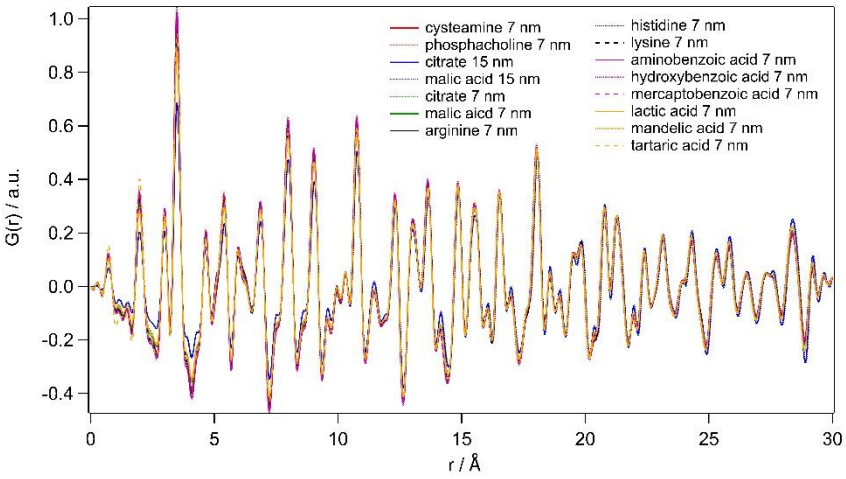

Supplementary Figure 10| Scaled powder pair distribution functions (PDF) of capped magnetic iron oxide nanopowders. The powder PDFs are scaled to 0.5 for the peak at 18.07 Å. All powders exhibit the same peaks indicating that only distances from the iron oxide nanocrystals are included and the ligand molecules cannot be seen in the PDF data herein.

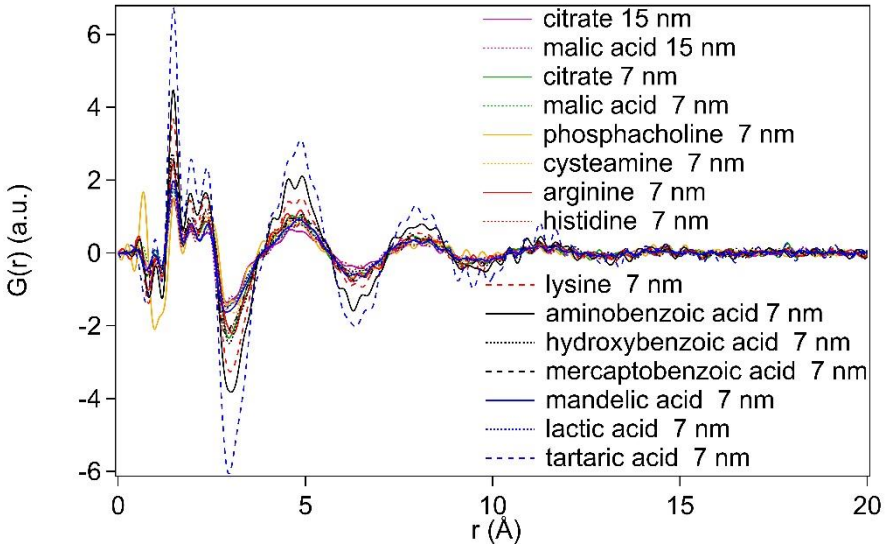

Supplementary Figure 11 | Comparison of hydration shells dependent on ligand. Scaled hydration shells (dd-PDFs) of differently functionalized and sized iron oxide nanoparticles evaluated for this work are shown in comparison. All samples exhibit the two discussed regimes – adsorption and hydration.

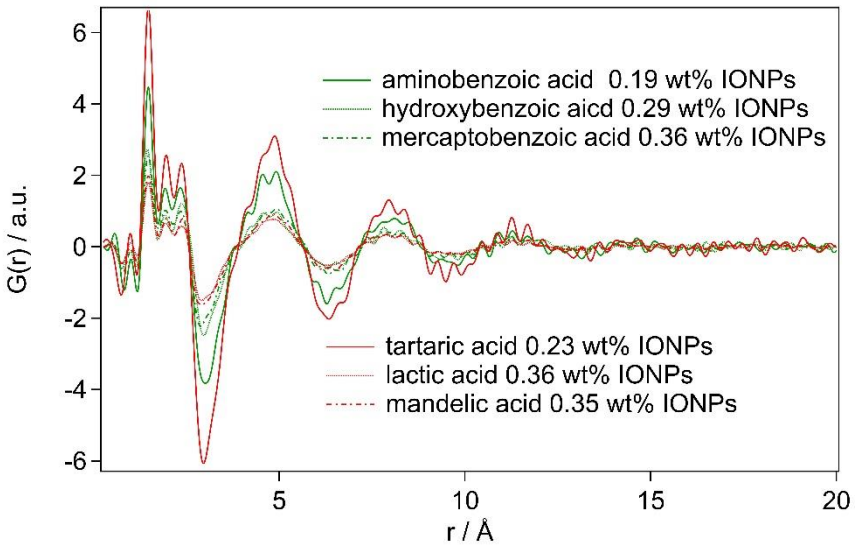

Supplementary Figure 12| Comparison of hydration shells dependent on concentration of nanoparticles in suspension. The signal of hydration shells (dd-PDFs) of some differently functionalized iron oxide nanoparticles (IONPs) are shown dependent on their concentration. The data indicate that a correlation of the amplitude of the hydration shell with the concentration exists. Samples with a lower IONP concentration (tartaric acid and aminobenzoic acid capped) exhibit a lower amplitude. Concentration dependent measurements of one sample (same ligand and size) are planned for the future.

Supplementary Tables

Supplementary Table 1 | TEM and DLS particle sizes, zetapotentials, concentrations of NP suspensions, together with ligand coverage from TGA.

sample	ξ [mV][	diameter DLS [nm]	diameter TEM [nm]	concentration [wt%]	ligand surface coverage [nm^{-2}]
citrate 15 nm	-32 ± 0.5	17.2 ± 0.7	15.0 ± 2.1	0.50	1.70
malic acid 15 nm	-35 ± 1.1	15.0 ± 0.2		0.30	3.11
citrate 7 nm	-35 ± 0.3	10.7 ± 0.2		0.38	1.92
malic acid 7 nm	-36 ± 0.8	8.5 ± 0.1		0.34	2.80
cysteamine 7 nm	38 ± 0.8	7.3 ± 0.2	6.8 ± 0.1	0.21	3.91
phosphacholine 7 nm	33 ± 0.5	6.1 ± 0.2	5.9 ± 1.8	0.31	1.00
arginine 7 nm	36 ± 1.1	6.7 ± 0.1		0.29	2.19
histidine 7 nm	31 ± 0.9	6.4 ± 0.3		0.27	1.79
lysine 7 nm	28 ± 0.6	6.4 ± 0.3	5.9 ± 0.9	0.30	1.80
aminobenzoic acid 7 nm	27 ± 0.5	8.0 ± 1.3		0.19	2.38
hydroxybenzoic acid 7 nm	-28 ± 0.9	6.0 ± 0.2	6.7 ± 0.3	0.29	2.36
mercaptobenzoic acid 7 nm	-33 ± 1.2	6.7 ± 0.2		0.36	3.05
lactic acid 7 nm	-36 ± 1.6	8.5 ± 0.1	7.4 ± 0.1	0.36	2.99
mandelic acid 7 nm	-30 ± 0.7	8.8 ± 0.1		0.35	2.04
tartaric acid 7 nm	-26 ± 1.1	9.8 ± 0.4		0.23	5.80

Supplementary Table 2 | Maxima positions of adsorbed water layer and hydration shell oscillations. Positions of three sharp peaks in comparison to the average value and the maxima of sinusoidal oscillation are listed.

Sample	Peaks of adsorbed water			Layers of hydration shell		
	1st [Å]	2nd [Å]	3rd [Å]	1st [Å]	2nd [Å]	3rd [Å]
citrate 15 nm	1.47	1.95	2.40	4.69	7.96	11.24
malic acid 15 nm	1.49	1.96	2.38	4.82	7.96	11.24
citrate 7 nm	1.47	1.93	2.35	4.69	7.96	11.24
malic acid 15 nm	1.49	1.96	2.38	4.69	7.96	11.24
cysteamine 7 nm	1.48	1.92	2.33	4.69	7.96	11.24
phosphacholine 7 nm	1.50	1.93	2.33	4.56	7.96	11.37
arginine 7 nm	1.47	1.91	2.33	4.69	7.96	11.24
histidine 7 nm	1.44	1.89	2.34	4.69	7.96	11.24
lysine 7 nm	1.47	1.92	2.34	4.69	7.96	11.24
aminobenzoic acid 7 nm	1.47	1.93	2.34	4.69	7.96	11.37
hydroxybenzoic acid 7 nm	1.45	1.92	2.37	4.69	7.96	11.37
mercaptobenzoic acid 7 nm	1.47	1.94	2.34	4.82	7.96	11.24
lactic acid 7 nm	1.47	1.94	2.37	4.69	7.96	11.24
mandelic acid 7 nm	1.48	1.96	2.39	4.69	7.96	11.24
tartaric acid 7 nm	1.48	1.95	2.37	4.69	7.96	11.24
average value	**1.48**	**1.95**	**2.39**	**4.70**	**7.96**	**11.27**